

Theoretical examination of the quantum-size effect in thin grey-tin films

B. I. Craig and B. J. Garrison

Department of Chemistry, The Pennsylvania State University, University Park, Pennsylvania 16802

(Received 2 October 1985)

A theoretical treatment of the thin-film size quantization of grey-tin is presented. The energy levels describing the band gap are calculated as a function of film thickness. The calculation employs the linear combination of atomic orbitals method to construct the appropriate wave functions and considers the effect of the surface and interface electronic structure. The results compare favorably with experiment. The band gap is found to have a maximum value of approximately 430 meV for a film thickness of 40 Å. The influence of the electronic structure due to the film boundaries is examined and shown to be important in order to examine the various experiments on the properties of the quantum-size effect.

I. INTRODUCTION

The electronic properties of thin solid films are currently receiving widespread attention. An important feature of the electronic structure is the quantum-size effect (QSE). This effect arises from the confinement of the electrons and holes to the film width. For films with thickness of 10–100 layers, the electronic structure is observed to be a manifold of subbands, rather than having the bulk band structure. Experiments with GaAs-Al_xGa_{1-x}As heterostructures^{1,2} have clearly demonstrated the existence of such quantum levels.

The qualitative nature of the splitting of the electronic structure into subbands can be easily described by the one-dimensional quantum square-well model. Each discrete level within the square well corresponds to the position of a subband within the manifold. A detailed analysis of the one-dimensional model was undertaken by Cottey in a series of papers.^{3,4} It was shown that for films of sufficient thickness the wave functions obtained from the square-well model are the envelope functions for the electron wave functions within the film. These envelope functions, like those of effective-mass theory, describe the contribution of the atomic orbital or Wannier functions at each unit cell within the crystal. Where the effective-mass function for a shallow level in a semiconductor is a hydrogeniclike function, the QSE envelope function has the form $\sin(n\pi z/L)$, where n is an integer and the film extends from $z=0$ to $z=L$.

The aim of this paper is to explore the nature of the quantum-size effect. This theoretical treatment will examine the recent experimental investigation of thin α -Sn films grown on a CdTe(111) surface.⁵ These experiments with high-resolution electron-energy-loss spectroscopy show an interesting finite band gap in α -Sn as a function of film thickness, in contrast to the zero band gap for a large crystal.

The linear combination of atomic orbitals (LCAO) method employed to calculate the electronic band structure of infinite solids⁶⁻⁸ is modified for the calculation of the electronic structure appropriate to a system of N atomic layers. This method gives the change in the ener-

gy levels describing the subband manifold edges as a smooth variation with N and therefore provides a useful method for calculating the change in band gap as a function of layer thickness. In addition, the nature of the wave functions corresponding to these energy levels is also described and compared with the predictions by the square-well model. As a result, a model for the plane-wave envelope within the thin film is developed with attention given to behavior of the wave functions near the surface and interface. This model is employed to examine the quantum-size experiments with thin-metal films,⁹ where small concentrations of impurities and defects at the surface or interface were shown to greatly distort the QSE.

The general theoretical background is established in Sec. II. The results are presented and discussed in Sec. III. Atomic units such that the unit of energy is the rydberg are used in this paper.

II. THEORY

The electronic structure for the thin film is obtained by the LCAO method. In general, this method gives the wave functions as

$$\Phi_{\alpha}(r) = \sum_{\mathbf{R}} \sum_i C_{i\mathbf{R}}^{\alpha} \phi_i(r - \mathbf{R}), \quad (1)$$

where $\phi_i(r - \mathbf{R})$ is the atomic orbital of type i , centered at site \mathbf{R} . The expansion coefficients $C_{i\mathbf{R}}^{\alpha}$ are obtained from the diagonalization of the Hamiltonian,

$$\sum_{i,\mathbf{R}} (H_{j\mathbf{R}',i\mathbf{R}} - E_{\alpha} S_{j\mathbf{R}',i\mathbf{R}}) C_{i\mathbf{R}}^{\alpha} = 0, \quad (2)$$

where S is the overlap matrix, and E_{α} is the energy level for state α . Equation (2) is usually solved numerically as a finite-matrix equation. Significant difficulties arise when comparing similar energy levels for systems with a different number of atomic sites as in the present problem where a change in film thickness is considered. The numerical difficulties arise from the changing basis and computational accuracy. In order to construct a method to examine the smooth change in the appropriate energy

levels from a change in film thickness, the properties of the wave functions describing the manifold edge are used.

In a three-dimensional crystal of N' unit cells ($N' \rightarrow \infty$) the band edge is described by a point \mathbf{k} within the three-dimensional Brillouin zone. The wave function for this state within the LCAO method is given by

$$\Phi_{n\mathbf{k}}(\mathbf{r}) = \sum_i \sum_{p=1}^{N_p} C_{i\mathbf{p}}^{\mathbf{k}} \Phi_{i\mathbf{k}}^p(\mathbf{r}), \quad (3)$$

where n is the band index and

$$\Phi_{i\mathbf{k}}^p = \frac{1}{(N')^{1/2}} \sum_{\mathbf{R}} \phi_i(\mathbf{r} - \mathbf{R} - \mathbf{R}_p) e^{i\mathbf{k} \cdot \mathbf{R}} \quad (4)$$

such that there are N_p atomic sites \mathbf{R}_p within each unit cell. In the LCAO method of Chadi⁶ and subsequent workers,^{7,8} the atomic orbitals $\{\phi_i(r)\}$ are chosen in order to fit known energy levels for a potential $V(\mathbf{r})$. A set of 10 Slater-type orbitals, whose exponents are computationally varied, have obtained an accurate description of the band structures of the diamond lattice structures, Si,⁷ Ge,⁸ and α -Sn.⁸ This set consists of an s orbital, a p orbital, and a d orbital, for all angular harmonics, and a single f orbital of the type $xyz \exp(-\beta r)$. For the specific case of α -Sn, $V(\mathbf{r})$ is the local pseudopotential of Cohen and Bergstresser.¹⁰ In the infinite crystal the overlap and Hamiltonian matrix elements are obtained from the following equations:⁷

$$\langle \Phi_{i\mathbf{k}}^p | \Phi_{j\mathbf{k}}^p \rangle = \Omega_{\text{BZ}} \sum_{\mathbf{g}} \alpha_i^*(\mathbf{k} + \mathbf{g}) \alpha_j(\mathbf{k} + \mathbf{g}) \times \exp[i(\mathbf{k} + \mathbf{g}) \cdot (\tau'_p - \tau_p)], \quad (5a)$$

$$\begin{aligned} \langle \Phi_{i\mathbf{k}}^p | H | \Phi_{j\mathbf{k}}^p \rangle &= \Omega_{\text{BZ}} \sum_{\mathbf{g}} \alpha_i^*(\mathbf{k} + \mathbf{g}) \alpha_j(\mathbf{k} + \mathbf{g}) |\mathbf{k} + \mathbf{g}|^2 \\ &\times \exp[i(\mathbf{k} + \mathbf{g}) \cdot (\tau'_p - \tau_p)] \\ &+ \sum_{\mathbf{g}, \mathbf{g}'} \alpha_i(\mathbf{k} + \mathbf{g}') \alpha_j(\mathbf{k} + \mathbf{g}) \\ &\times \cos[(\mathbf{g}' - \mathbf{g}) \cdot \boldsymbol{\tau}] V(\mathbf{g}' - \mathbf{g}) \\ &\times \exp\{i[(\mathbf{k} + \mathbf{g}') \cdot \tau'_p - (\mathbf{k} + \mathbf{g}) \cdot \tau_p]\}, \end{aligned} \quad (5b)$$

where $\boldsymbol{\tau} = (a/8, a/8, a/8) = \boldsymbol{\tau}_1 = -\boldsymbol{\tau}_2$. The functions $\Phi_{i\mathbf{k}}^p$ are given by Eq. (4) and $\alpha_i(q)$ is the Fourier transform of the atomic orbital $\phi_i(r)$.

With α -Sn, the \mathbf{k} point describing the band gap is the Γ point ($\mathbf{k} = 0$) for both the valence maximum and the conduction-band minimum. As α -Sn is a zero-gap semiconductor, these energy levels have the same value. However, in a crystal of fine thickness (N layers), in the (111) direction, the three-dimensional Brillouin zone (k_x, k_y, k_z) is replaced by a two-dimensional zone (k'_x, k'_y), where

$$k'_x = (1/\sqrt{2})(k_x - k_z), \quad k'_y = (1/\sqrt{6})(k_x - 2k_y + k_z).$$

In addition, each band n is described by a manifold of N subbands, characterized by a quantized wave number

$$k'_z = (1/\sqrt{3})(k_x + k_y + k_z) = m\pi/L.$$

For N sufficiently large the band edge is described by $m=1$ and the Γ point of the two-dimensional Brillouin zone $\mathbf{k}' = (0,0)$. The wave function for this state is written as a sum over layers, namely

$$\phi_\alpha(\mathbf{r}) = \sum_{\lambda_p} \sum_i C_{i\lambda_p}^\alpha \Phi_i(\mathbf{r} - \lambda_p), \quad (6)$$

where $\Phi_i(\mathbf{r} - \lambda_p)$ is an intralayer sum over N_L lattice sites \mathbf{R} within the (111) layer and is given by

$$\Phi_i(\mathbf{r} - \lambda_p) = \frac{1}{(N_L)^{1/2}} \sum_{\mathbf{R}} \phi_i(\mathbf{r} - \mathbf{R} - \lambda_p),$$

where there are N_L atoms with each (111) layer p , and λ_p is the translation vector of the p th layer from the surface layer ($\lambda_1 = 0$). The coefficients $C_{i\lambda_p}^\alpha$ describe the contribution of the orbitals ϕ_i within the p th layer to the state α . For layers not too near the crystal faces, these coefficients for the manifold edge ($m=1$) have the form^{3,4}

$$C_{i\lambda}^\alpha = \left[\frac{2}{N} \right]^{1/2} \sin \left[\left| \lambda_{p,z'} \right| \frac{\pi}{L} \right], \quad (7)$$

where $\lambda_{p,z'}$ is the component of λ_p in the direction normal to the film surface. Near the surface there exists a surface-localized electronic structure not simply described by the one-dimensional square-well model. Included in this surface-electronic structure are surface states and resonances which are, of course, orthogonal to the manifold edge states. Therefore, for layers p near the crystal edges (or film boundary) the coefficients $C_{i\lambda_p}^\alpha$ may vary significantly from the form given by Eq. (7).

A method for describing the energy level of the manifold edge can be obtained by choosing the following lattice sums as basis functions for the matrix diagonalization, instead of the entire crystal's sums for the three-dimensional crystal. For layers $p=1$ to N_s and from $N - N_s$ to N the functions $\Phi_i(\mathbf{r} - \lambda_p)$ for each i are included to describe the effect of the surface-electronic structure, while for the remaining region of the film [layers $p = N_s + 1$ to $N - (N_s + 1)$] only two summations for each i are used. These summations are

$$\Psi_i^{(1)}(\mathbf{r}) = \frac{1}{(N)^{1/2}} \sum_p \sin \left[\left| \frac{\lambda_{pz}}{L} \right| \pi \right] \Phi_i(\mathbf{r} - \lambda_p) \quad (8a)$$

and

$$\begin{aligned} \Psi_i^{(2)}(\mathbf{r}) &= \frac{1}{(N)^{1/2}} \sum_p \sin \left[\frac{\pi}{L} \left| (\lambda_p + \mathbf{R}_e)_z \right| \right] \\ &\times \Phi_i(\mathbf{r} - \lambda_p - \mathbf{R}_e), \end{aligned} \quad (8b)$$

where $\mathbf{R}_e = (a/4, a/4, a/4)$ and describes the translation vector between the two Sn atoms belonging to the fcc unit cell. N_s is the number of surface layers in which the coefficients $C_{i\lambda}^\alpha$ are allowed to vary. In the current treatment $N_s = 5$. The summations \sum_p within Eqs. (8a) and (8b) give a layer sum over the fcc (111) layer structure and do

not include the surface layers. These two layer summations, $\Psi^{(1)}$ and $\Psi^{(2)}$, describe the contribution from each Sn atom within the fcc unit cell.

The expansion coefficients $C_{\alpha_i}^{(1)}$ and $C_{\alpha_i}^{(2)}$ obtained from the matrix diagonalization therefore describes the bonding and antibonding character for each orbital i within each state α . As an example, coefficients with values $C_s^1 = C_s^2$ describes the s bonding state, while $C_s^1 = -C_s^2$ describes the s antibonding state. The sine form [Eq. (7)] for the coefficients $C_{i\lambda}^\alpha$ for these layers has been assumed. The matrix elements for the Hamiltonian and the overlap matrices for these basis functions are obtained from the matrix elements between the single (111)-layer summations, $\Phi_j(\mathbf{r}-\lambda)$.

The matrix elements for those (111)-layer summations over a three-dimensional Hamiltonian are given by

$$S_{ij}(\lambda) = \langle \Phi_i(\mathbf{r}) | \Phi_j(\mathbf{r}-\lambda) \rangle \\ = \frac{\Omega_{\text{BZ}}}{N_q} \sum_{\mathbf{q}} \sum_{\mathbf{g}} \alpha_i^*(\mathbf{q}+\mathbf{g}) \alpha_j(\mathbf{q}+\mathbf{g}) e^{-i(\mathbf{q}+\mathbf{g})\cdot\lambda}, \quad (9)$$

$$T_{ij}(\lambda) = \langle \Phi_i(\mathbf{r}) | -\nabla^2 | \Phi_j(\mathbf{r}-\lambda) \rangle \\ = \frac{\Omega_{\text{BZ}}}{N_q} \sum_{\mathbf{q}} \sum_{\mathbf{g}} \alpha_i^*(\mathbf{q}+\mathbf{g}) \alpha_j(\mathbf{q}+\mathbf{g}) |\mathbf{q}+\mathbf{g}|^2 \\ \times e^{-i(\mathbf{q}+\mathbf{g})\cdot\lambda}, \quad (10)$$

$$V_{ij}(\lambda) = \langle \Phi_i(\mathbf{r}) | V(\mathbf{r}) | \Phi_j(\mathbf{r}-\lambda) \rangle \\ = \frac{\Omega_{\text{BZ}}}{N_q} \sum_{\mathbf{q}} \sum_{\mathbf{g}} \sum_{\mathbf{g}'} \alpha_i^*(\mathbf{q}+\mathbf{g}') \alpha_j(\mathbf{q}+\mathbf{g}) e^{-i(\mathbf{q}+\mathbf{g})\cdot\lambda} \\ \times V(\mathbf{g}'-\mathbf{g}) \cos[(\mathbf{g}'-\mathbf{g})\cdot\boldsymbol{\tau}] \\ \times e^{-i(\mathbf{g}'-\mathbf{g})\cdot\boldsymbol{\tau}}, \quad (11)$$

and $\boldsymbol{\tau} = (a/8, a/8, a/8)$, where $\sum_{\mathbf{q}}^{N_q}$ is a sum over points in the three-dimensional Brillouin zone, in the interval $(-\pi/a, \pi/a, \pi/a)$ to $(\pi/a, \pi/a, \pi/a)$.

Using these equations, the matrix elements between the 120 basis functions can be constructed. The film thickness is controlled by the choice of the value for N describing the layer sums [Eqs. (8)]. The orbitals belonging to the surface layers feel the effect of the surface potential. In this current work the surface potential is described by a model potential,

$$V_s(\mathbf{r}) = \begin{cases} V_0 \left[\frac{(z-z_0)^2}{(1+(z-z_0)^2)} \right] + V(\mathbf{r}) \frac{1}{[1+(z-z_0)^2]} \\ \text{for } z > z_0, \\ V(\mathbf{r}) \text{ for } z < z_0, \end{cases} \quad (12)$$

where $V(\mathbf{r})$ is the bulk potential and $z=0$ describes the first layer. The vacuum is described by $z>0$ and z_0 occurs just outside the first layer. The potential matrix elements for the near-surface orbitals therefore need to be

corrected by the additional term

$$\langle \Phi_i(\mathbf{r}-\lambda) | \frac{(z-z_0)^2}{1+(z-z_0)^2} [V_0 - V(\mathbf{r})] | \Phi_j(\mathbf{r}-\lambda') \rangle, \quad (13)$$

which is obtained by a real-space integration for $z > z_0$. As only the tails of these orbitals see the surface potential, the form for $V_s(\mathbf{r})$ for large z is not important, and the additional term is not large. The electronic structure for the film is therefore solved for a system of N layers of atoms embedded in a potential well. The potential well is modeled by $V_0=0.8$ Ry (the sum of E_F and the work function), while z_0 was chosen to be 0.3 of the Sn nearest-neighbor distance. This choice of potential gives only a qualitative model for the real surface potential. The system is not sensitive to the details of the choice of this potential, but mainly depends on the atomic wells in which the orbitals are embedded. The results in the next section show no large changes in the energy levels when comparing the system with this surface potential to one where it is neglected.

This method therefore gives an approximate description of the surface-electronic structure. The method is not self-consistent and employs the same model potential for both the surface and the film-substrate interface in order to maintain the central symmetry for the film in the (111) direction. Fortunately, these boundary layers give only a very small contribution to the layer summation for the band manifold edge states [Eq. (7)].

The most important feature not considered in this method is the effect arising from the surface- (and the interface-) layer relaxation and reconstruction. This would lead to larger changes in the Hamiltonian matrix elements and therefore may yield possible significant changes in the electronic structure in the surface (and interface) region. However, no experiment or theory has determined the nature of the surface- and interface-layer reconstruction, and therefore a precise knowledge of the surface-electronic structure cannot be obtained. The current work obtains a basic model for the α -Sn (111) film and yields an illustrative example for the electronic structure rather than an accurate self-consistent calculation for the system corresponding to the experiment, which due to the large uncertainty arising from the surface reconstruction, cannot be obtained.

III. RESULTS AND DISCUSSION

The energy levels for the subband manifold edges have been calculated by the theory outlined in the preceding section. The change in the energy levels as a function of the film thickness are shown in Fig. 1. This figure shows the energy levels for films with and without the inclusion of the surface potential ($V_0=0.8$, $z_0=0.3$). In addition, the energy-level curve for a square well, namely $E = (1/M_x)(\pi/L)^2$ is also displayed for effective masses, 0.23 and 0.0236, equal to the valence- (hole) and conduction- (electron) band values, respectively.⁵ Good agreement is obtained for the valence curve but not for the conduction curve. These results can be understood by examining the nature of the wave functions for each level.

The energy levels displayed in Fig. 1 can be denoted the

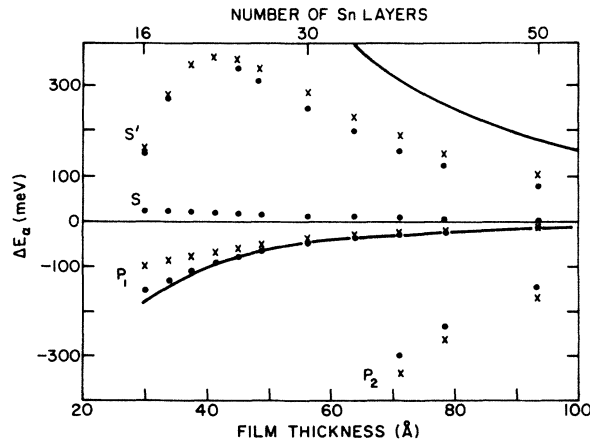


FIG. 1. Graph of the change in the energy levels ΔE_α , from the values for a film with infinite thickness, as a function of film thickness. The levels shown are the bonding and antibonding s levels (s and s' , respectively), the p level aligned in the $[111]$ direction, denoted by P_2 , and the doubly degenerate p level (P_1) with p orbitals aligned in the $[10-1]$ and $[1-21]$ directions. The values of ΔE_α given by crosses and solid circles are for films with and without the inclusion of the surface potential, respectively. The simple effective-mass values are shown as solid curves.

s bonding level (E_s), the s antibonding level (E'_s), the $(p_x + p_y + p_z)$ level ($E_{(111)}$), and the doubly degenerate p levels, $E_{(10-1)}$ and $E_{(1-21)}$, describing the $p_x - p_z$ and $p_x - 2p_y - p_z$ combinations of the p orbitals. The s bonding and antibonding levels describe the bottom of the valence and conduction manifolds, respectively, while the degenerate p levels, $(10-1)$ and $(1-21)$, describe the top of the valence manifold. Along with each of the three p states are contributions from the d orbitals, such that the coefficients of the d_{yz} , d_{xz} , and d_{xy} orbitals are approximately 0.25 of the p_x -, p_y -, and p_z -orbital coefficients, respectively. Similarly, the f_{xyz} orbital contributes to the s antibonding orbital with a coefficient of 0.05–0.15 of the s coefficient. This coupling is, of course, due to the xyz symmetry about each lattice site.

For large film thickness (small wave number) the energy levels qualitatively behave like the bulk band structure for α -Sn in the Γ - L direction within the three-dimensional Brillouin zone,⁸ where the wave number $k = (\pi/\sqrt{3}L)(1,1,1)$. This result is expected as the contribution from the perturbed surface-electronic structure is not sufficiently great to distort the envelope function for large L . In this case the envelope function looks like

$$C(\mathbf{R}) = \sin(\mathbf{k} \cdot \mathbf{R}) = \frac{1}{2i}(e^{i\mathbf{k} \cdot \mathbf{R}} - e^{-i\mathbf{k} \cdot \mathbf{R}}) \quad (14)$$

for most lattice sites \mathbf{R} . The band-edge states for the film qualitatively look like a combination of the degenerate Bloch functions $\phi_{\mathbf{k}}(\mathbf{r})$ and $\phi_{-\mathbf{k}}(\mathbf{r})$ of the infinite crystal, and therefore an energy level $E(\mathbf{k})$ belonging to the Γ - L interval of the three-dimensional Brillouin zone.

In the infinite crystal⁸ the three p levels are degenerate at the Γ point (Γ_{25} level). Along the interval from the Γ

point $(0,0,0)$ to the L point $(\pi/a, \pi/a, \pi/a)$, the degeneracy is split into the $E_{(111)}$ level, which decreases rapidly, while the levels $E_{(10-1)}$ and $E_{(1-21)}$ decrease more slowly, like $E_k = (1/M_h)|\mathbf{k}|^2$. The s antibonding level ($\Gamma_{2'}$) however, behaves as $(1/M_e)|\mathbf{k}|^2$ for only small $|\mathbf{k}|$ and departs from the parabolic behavior with increasing \mathbf{k} such that the energy level obtains a maximum at $\mathbf{k} \approx \frac{1}{4}(\pi/a, \pi/a, \pi/a)$.

When considering the case of a film, the truncation of the number of layers leads to a severe perturbation. This perturbation has its greatest effect on those states where the orbitals from adjoining layers overlap significantly. The $(p_x + p_y + p_z)$ level describes a p orbital aligned in the $[111]$ direction, normal to each layer. Similarly, the s states require orbitals on the next layer to construct the antibonding combination. However, in the case of the degenerate p levels, the orbitals $(p_x - p_z)$ and $(p_x - 2p_y - p_z)$ describe p orbitals aligned parallel to the surface, localizing the wave function within each layer and reducing the sensitivity of this level to interlayer perturbations. The good agreement between these p levels and the simple parabolic form shown in Fig. 1 is therefore not surprising.

In addition to the disagreement between the level E'_s and the parabolic form employing the bulk effective mass, the maximum in this level is achieved at a thickness corresponding to the wave number $\mathbf{k} \sim \frac{1}{12}(\pi/a, \pi/a, \pi/a)$. This wave number is approximately one-third of the value suggested by the bulk band structure. These features for E'_s demonstrate the sensitivity of this level to the perturbation arising from the surface and interface.

A surface state was found to exist. The energy level for this state was determined to be 0.5 eV below the Fermi energy E_F for the film including the surface potential and close to E_F without the surface potential. These energy levels have significant uncertainties due to the limited size of the basis employed and the lack of self-consistency which, although adequate to describe the states within the crystal potential, is possibly insufficient to accurately describe the electronic structure arising from the introduction of the surface potential.

This surface state is localized to the first four layers. The energy level does not change significantly with the film size, which is, of course, a property of the surface-localized state. The energy variation is of the order of 10^{-3} eV for $L = 30$ –300 Å. The state can be qualitatively described as a hybridization between an antibonding s state in the first two layers (where each Sn atom in the first layer has three nearest neighbors on the second layer) and p orbitals aligned in the $[111]$ direction. The mixing of the p (111) orbitals with the antibonding s state varies with the surface potential. The existence of this surface state, and the surface-electronic structure in general, leads to a variation in the coefficients C_{λ}^{α} [Eq. (7)] from the simple "sine" form for the first four layers. The variation results from the orthogonality of the band-edge states to the surface states and resonances. The coefficient for the fifth layer agrees with the "sine" expression by approximately $\pm 20\%$ or better for the band-gap levels $E_{(10-1)}$, $E_{(1-21)}$, and E'_s , and a film thickness of $L > 30$ Å. This feature is not surprising as the surface state has little contribution from the fifth layer. The s bonding level (E_s),

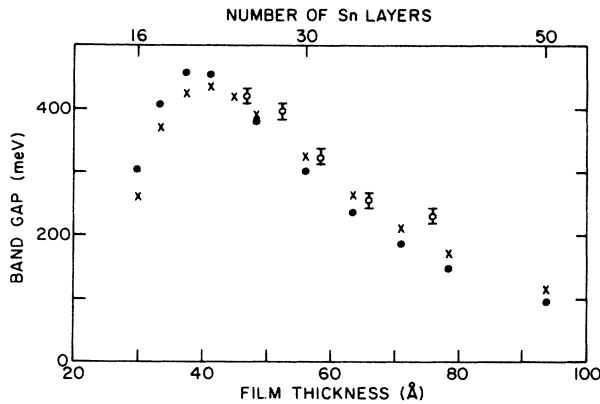


FIG. 2. Graph of the band gap as a function of film thickness. The values given by crosses and solid circles are the theoretical values for films with and without the inclusion of the surface potential, respectively. The experimental values (Ref. 5) are given by the open circles.

however, shows reasonable agreement for all layers where, due to the antibonding s nature of the surface state, little adjusting is required to maintain orthogonality.

In Fig. 2 the band gap is displayed as a function of film thickness. It can be readily seen that the effect of including the surface potential, describing a greater perturbation in the surface region, is to improve the agreement with the experimental results.⁵ For large thickness the surface potential has the effect of increasing the band gap, while at $L < 50$ Å the inclusion of the surface potential results in a greater departure from the parabolic form suggested by the one-dimensional model.

The experimental results indicate that the surface and interface undergo a greater perturbation than is modeled by the current simple method. The experiment yields a greater band gap at $L > 60$ Å while the departure from the parabolic form seems to occur at approximately 5–10 Å larger thickness than suggested by the simple surface potential. These results are not surprising as surface and interface reconstruction has been neglected and therefore this larger perturbation could quite easily yield this result.

An extension of the square-well model to incorporate the finite surface and interface potential barriers and step functions along the lines of earlier work⁵ is not considered here as an accurate description of the effect of the surface and interface. This approach solves the one-dimensional wave equation for a finite-well system, obtaining the appropriate eigenvalues and eigenfunctions. However, rather than describing the electron wave functions, the sine wave functions obtained from the square-well model qualitatively describe the coefficient of the Wannier function or atomiclike orbital at each site. It is the tail of each orbital (multiplied by the coefficient) which senses these potential barriers, rather than the smoothly varying sine function, which would have a greater magnitude in the barrier region. The confinement of these electron states by the atomic wells at the surface and interface, in addition to the film potential well, therefore, needs to be considered. The results presented here show that the per-

turbed electronic structure within the surface (interface) layers arising from the surface (interface) reconstruction is an important additional feature of the film boundary in examining the confinement of states to a single potential well. In a more general situation where the states may have sufficient energy to occur above the potential barriers, as in the case of very-low-energy electron diffraction within thin metal films,^{9,11} or heterostructures where there is an array of potential wells (and therefore tunneling),^{1,2} the potential beyond each single well needs careful consideration along with the interface-localized structure in order to obtain a quantitative description of the electronic behavior.

The square-well approach can be followed in analyzing some of these results by including the contribution from the surface-electronic structure. In the simple model the square-well functions $\phi_i(z)$ and the layer coefficients are given by the plane-wave form

$$\phi_i(z) = \sin \left[\frac{\pi z}{L} \right], \quad C_i(\lambda) = \sin \left[\frac{\pi}{L} |\lambda_z| \right].$$

A generalized treatment considers a plane-wave function $|\text{PW}, K\rangle$, where in the above specific case $K = \pi/L$. In the general case $K \approx n\pi/L$ for bound states and is continuous for states above the well, but here attention is restricted to the nature of these wave functions within the region of the film. Including the orthogonality of these wave functions with the surface (interface) electronic structure, the coefficients $C_i(\lambda)$ are related to an orthogonalized plane function $|\text{OPW}, K\rangle$. The two functions can be expressed by the equation

$$|\text{OPW}, K\rangle = |\text{PW}, K\rangle + \sum_s \beta_{sK} |\psi_s\rangle, \quad (15)$$

such that

$$\beta_{sK} = -\langle \psi_s | \text{PW}, K \rangle, \quad (16)$$

and the functions $|\psi_s\rangle$ are the states within the surface-electronic structure. As $|\psi_s\rangle$ and $|\text{OPW}, K\rangle$ are eigenstates of the realistic model of the system, then

$$H |\psi_s\rangle = E_s |\psi_s\rangle, \quad H |\text{OPW}, K\rangle = E_K |\text{OPW}, K\rangle, \quad (17)$$

where

$$H = -\nabla^2 + V(r). \quad (18)$$

This approach of course follows from the orthogonalized-plane-wave (OPW) method widely used in pseudopotential theory.¹² The usual OPW equation is obtained by substituting Eqs. (15) and (18) into (17), giving

$$[-\nabla^2 + V(r) + V^{\text{OPW}}] |\text{PW}, K\rangle = E_K |\text{PW}, K\rangle, \quad (19)$$

where

$$V^{\text{OPW}} = \sum_s (E_K - E_s) |\psi_s\rangle \langle \psi_s|. \quad (20)$$

Therefore, plane waves $|\text{PW}, K\rangle$ appear to be scattered by a potential $V(r) + V^{\text{OPW}}$ which has a more "square-well-like" form than the potential $V(r)$. Any model surface potentials which yield good agreement with experiment in terms of the scattering of plane waves include the contri-

bution of V^{OPW} and are therefore a type of pseudopotential.

This OPW approach can be used in examining the experiments looking at the scattering of plane-wave states at the surface and interface barriers of thin films. Experiments with (111) layers of Cu and Ag grown on a W(110) substrate show distinct quantum-size effects in the scattering of low-energy electrons, where the eigenvalues E_K occur above the barrier. Various model potentials for the surface barriers within the one-dimensional model have been examined in order to describe the experimentally observed quantum-size oscillations.^{9,11} However, the most interesting result with regard to the above OPW approach is the sensitivity of this quantum-size effect to defects within the surface or interface. Both impurities (oxygen and carbon) and lattice defects (described by a step atom density) were used to create the perturbed surfaces. At the vacuum-film interface a step atom density of 6.5% decreased the magnitude of the observed oscillations by a factor of 2, while 12% coverage removed the oscillations. At the film-substrate interface an increase of the step atom density from 1% to 3% decreased the magnitude of the oscillations by 70%. The OPW potential [Eq. (20)] is strongly dependent on the electronic structure at each interface. A defect at the surface or interface will not only affect the electronic structure localized to the central site but also the neighboring atoms according to the change in the lattice reconstruction or surface states describing dangling bonds. This enhancement in the surface area of the perturbation would therefore be the order of the number of nearest neighbors, equal to 6 for a fcc (111) surface. The plane waves operated on by the OPW potential would therefore sense different potentials for each region and

lead to destructive interference and dampening on the oscillations as a function of K . The level of dampening depends on the strength of the perturbation in V^{OPW} with respect to $V(r)$ and the relative area of the perturbed region. With the interface potential barrier being smaller than surface barrier, and the observed perturbations arising from defect concentrations of the order of 5%, this theoretical approach is consistent with these experimental results.

IV. CONCLUSION

The general behavior of the film-thickness-dependent band gap in thin (111) grey-tin films has been adequately described by the LCAO method. The calculations show a maximum value for the band gap at thickness approximately equal to 40 Å, in contrast to the simple one-dimensional model where no maximum should occur. This feature results from the localized electronic structure at both the surface and the film-substrate interface. A detailed treatment for obtaining an accurate calculation of this electronic structure requires a precise knowledge of the lattice reconstruction at these film boundaries, which at present is unfortunately not known. However, the work presented here provides a useful illustrative example of thin-film confinement through the consideration of the three-dimensional nature of the system.

ACKNOWLEDGMENTS

The financial support of the U.S. Office of Naval Research, the National Science Foundation, the IBM Corporation, and the Camille and Henry Dreyfus Foundation (New York, NY) is gratefully acknowledged.

¹L. L. Chang, K. Esaki, and R. Tsu, *Appl. Phys. Lett.* **24**, 593 (1974).

²R. D. Dingle, W. Wiegmann, and C. H. Henry, *Phys. Rev. Lett.* **33**, 827 (1974).

³A. A. Cottey, *J. Phys. C* **6**, 2446 (1975).

⁴A. A. Cottey, *Phys. Status Solidi B* **88**, 207 (1978).

⁵S. Takatani, and Y. W. Chung, *Phys. Rev. B* **31**, 2290 (1985).

⁶D. J. Chadi, *Phys. Rev. B* **16**, 3572 (1977).

⁷M. Downey and P. V. Smith, *Phys. Status Solidi B* **115**, 255 (1983).

⁸P. V. Smith, *Phys. Status Solidi B* **116**, 101 (1983).

⁹B. T. Jonker, N. C. Bartlett, and R. L. Park, *Surf. Sci.* **127**, 183 (1983); B. T. Jonker and R. L. Park, *ibid.* **146**, 93 (1984); **146**, 511 (1984).

¹⁰M. L. Cohen and T. K. Bergstresser, *Phys. Rev.* **141**, 789 (1966).

¹¹H. Iwasaki, B. T. Jonker, and R. L. Park, *Phys. Rev. B* **32**, 643 (1985).

¹²V. Hiene, in *Solid State Physics*, edited by F. Seitz, D. Turnbull, and H. Ehrenreich (Academic, New York, 1970), Vol. **24**, p. 1.